Shelving Filter Cascade with Adjustable Transition Slope and Bandwidth

Frank Schultz, Nara Hahn, Sascha Spors

Institute of Communications Engineering, University of Rostock

Rostock, Germany

{frank.schultz, nara.hahn, sascha.spors}@uni-rostock.de

Abstract—A shelving filter that exhibits an adjustable transition band is derived from a cascade of second order infinite impulse response shelving filters. Two of three parameters, i.e. shelving level, transition slope and transition bandwidth, can be freely adjusted in order to describe the design specifications. The accuracy of the resulting response depends on the number of deployed biquads per octave. If this is set too small, deviations in level and bandwidth as well as a rippled slope can occur. The shelving filter cascade might be used in applications, that require a fractional-order slope in a certain bandwidth, such as for sound reinforcement system equalization, sound field synthesis and audio production.

Index Terms—shelving filter, shelving filter cascade, shelving bandwidth, shelving slope, transition band, fractional-order slope

I. Introduction

Equalizers (EQs) [1] are fundamental tools for audio signal processing, more precisely for filtering, where spectra of audio signals are intentionally reshaped. For traditional shelving filters [2–5], realized as infinite impulse response (IIR) filters, cutoff frequency, shelving level and Q-factor are design specifications and determine the placement of M poles and M zeros. The steepness of the slope is typically linked to level. For practical levels, a somewhat steeper or flatter slope can be realized at the cost of frequency responses that are underdamped (large Q) or overdamped (small Q), respectively. For the mentioned filter designs of order M, the transition slope and bandwidth are not independently adjustable and for large levels the slope is always restricted to $\pm 6 \cdot M$ dB/oct, cf. [6]. However, the slope and bandwidth of the transition band can be considered as design specifications, cf. [7]. Fractional-order system theory allows to design filters with arbitrary slope ν dB/oct ($\nu \in \mathbb{R}$) [8, 9]. The intended accuracy of the slope determines the required IIR filter order M. A suitable filter design determines their specific alignment. By that shelving filters could be enhanced for separate adjustment of shelving level and arbitrary slope or lower/upper cutoff frequencies (determining the bandwidth of the slope). A finite impulse response (FIR) filter design is straightforward. However, standard FIR designs exhibit a linear frequency scale. Thus, control of low frequencies requires a rather long impulse response and comparably high computational complexity. This might be lowered by a cascade of IIR filters with inherent minimum phase. The slope of

a fractional-order filter and particular its minimum phase characteristic is a desired property in certain audio applications [7, 10].

In [11] a cascade design of second-order shelving filters with ± 3 dB/oct slope was introduced, to approximate the frequency response of the so called half-differentiator/-integrator (± 45 deg minimum phase) within certain bandwidth. Hélie [8] recently introduced a fractional-order lowpass filter design from parallel connection of poles. The treatise gives the theoretical link to the so called diffusive representation, which represents the transfer function of a fractional-order lowpass as an integral over infinite, infinitesimally shifted poles. Approximating this integral by a finite sum leads to a parallel filter structure. This can be converted to a cascade [12]. The usage of a finite number of poles introduces ripples to the ideal fractional-order slope. In the present contribution, a shelving filter cascade upon this fundamental concept is designed as generalization of [11] towards a shelving filter with arbitrary fractional-order slope and adjustable bandwidth. The approach thus explicitly controls the transition band and could not be traced in literature, but naturally there are strong links to other filter design concepts. These will be briefly outlined in the following.

Research on (digital) fractional-order filter design is particularly pursued in control engineering, cf. [13–16]. These IIR filter designs approximate a fractional-order system and pay special attention to the optimum slope and phase in a specified bandwidth. This often comes at the cost of disregarded shelving bands, which might exhibit arbitrary magnitude, phase and/or ripple. The low-order -3 dB/oct fractional-order slope lowpass IIR filters collected in [17] are popular in audio engineering, e.g. to create pink from white noise.

Furthermore in audio, a cascade of parametric EQs (PEQs) or shelving filters is often pursued, typically to obtain a graphical EQ (GEQ) [18, 19] or a parametric multiband EQ [7, 20–22]. In [7] adjustable fractional-order slope and bandwidth was introduced to shelving filters for loudspeaker controllers. Using a raised-cosine slope—approximated by a PEQ cascade—enhanced the capabilities to equalize sound reinforcement systems. Higher-order shelving slopes without excessive under-/overdamping can be achieved by higher-order shelving filters [6]. This does not allow to design the slope explicitly, but it is linked to the level and the filter order, as stated before. An

example for this characteristic is depicted in Fig. 7 in the present paper. The design in [6] allows for band-shelving filters with steep transition between the pass band and the shelving band. In [18] this was used to design a GEQ with a cascade of sharp band-shelving filters. With [6, 18] the multiband EQ described in [22] can be straightforwardly designed: A customized cascade is used to realize multiple band-shelving filters, where asymmetric slopes are linked to level and filter order. Similar to [7] this design enhances capabilities for sound reinforcement system equalization. A further design [20, 21] uses cascaded fractional-order shelving filters to obtain a shelving filter with adjustable lower and upper cutoff frequency and corresponding levels. By that a transition bandwidth is explicitly defined. The slope is optimized such that an intended sharpness in the transition band is suitable for a target application. For their fractional-order shelving prototypes, the works [20, 21] use the fact, that a certain integer order shelving filter with a certain chosen level yields a specific fractional-order slope in a limited bandwidth.

In comparison to the mentioned multiband EQs, our paper aims at shelving filters with adjustable fractional-order slopes over a larger bandwidth, for which the resulting minimum phase can be useful in certain applications. The paper is thus organized as follows: In Sec. II the filter design method and parametrization is discussed. In Sec. III the tuning and limitation properties of the analog filter type are explained in detail. In Sec. IV digital filter design, comparison to a digital GEQ design and potential applications are discussed. Sec. V briefly summarizes the outcome. All source code[1] to this paper is available.

II. FILTER DESIGN METHOD

The analog filter design found e.g. in [1, Sec. 3.2], [23] is used to realize shelving filters with mid-level cutoff frequency definition. This is known as *one-half-pad loss* filter characteristic [2]. For convenience the resulting filter coefficients for 1st/2nd low-/high-shelving filters are reviewed in the Appendix. The discussion of the filter design method concentrates on the cascade of 2nd order low-shelving filters in the remainder. Cascading high-shelving filters is straightforward.
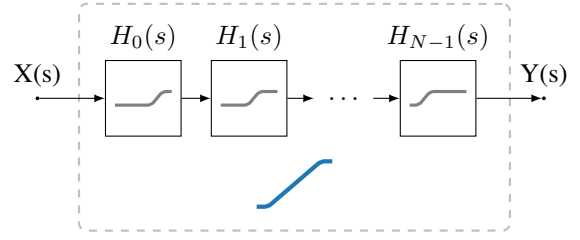
A. Cascade of 2nd Order Low-Shelving Filters

The cascade (i.e. the series connection) of N 2nd order filters (biquads) is given as transfer function
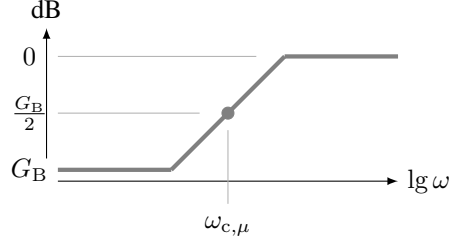
$$H(s) = \frac{Y(s)}{X(s)} = \prod_{\mu=0}^{N-1} H_\mu(s) \tag{1}$$

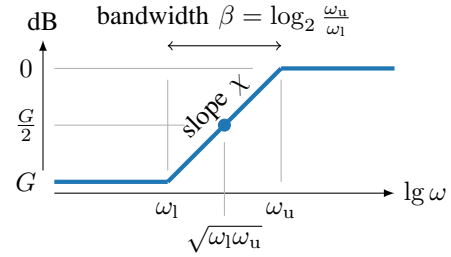in Laplace domain, being sketched in Fig. 1a. The μ-th biquad of the cascade is defined as, cf. (12)

$$H_\mu(s) = \frac{b_{2,\mu}\, s^2 + b_{1,\mu}\, s + b_{0,\mu}}{a_{2,\mu}\, s^2 + a_{1,\mu}\, s + a_{0,\mu}}, \tag{2}$$

(a) Signal flow for shelving filter cascade with input $X(s)$, output $Y(s)$ and biquads $H_\mu(s)$ in series in the Laplace domain.

(b) Level response $20 \lg |H_\mu(\omega)|$ of low-shelving biquad for $G_B < 0$ and mid-level cutoff frequency $\omega_{c,\mu}$.

(c) Level response $20 \lg |H(\omega)|$ of shelving filter cascade for $G < 0$ and lower/upper cutoff frequency $\omega_{l/u}$. For a dedicated ω_u, additionally two of the three parameters χ, β and G can be freely adjusted.

Fig. 1: Signal-flow graph (a) and schematic level responses of a single 2nd order shelving filter (b) and the proposed shelving filter cascade (c).

with the corresponding coefficients, cf. (15)

$$b_{2,\mu} = \frac{1}{\omega_{c,\mu}^2}, \quad b_{1,\mu} = \frac{g_B^{\pm\frac{1}{4}}}{Q\,\omega_{c,\mu}}, \quad b_{0,\mu} = g_B^{\pm\frac{1}{2}}, \tag{3}$$

$$a_{2,\mu} = \frac{1}{\omega_{c,\mu}^2}, \quad a_{1,\mu} = \frac{g_B^{\mp\frac{1}{4}}}{Q\,\omega_{c,\mu}}, \quad a_{0,\mu} = g_B^{\mp\frac{1}{2}},$$

with mid-level cutoff frequency $\omega_{c,\mu}$ in rad/s and the pole/zero Q-factor. The required gain parameter $g_B = 10^{|G_B|/20} > 0$ is derived from the biquad shelving level G_B in dB. The $\pm$ exponent corresponds to positive/negative G_B. The biquad shelving level G_B is determined by the filter design algorithm in (8). While G_B and the user definable Q-factor are held constant for all μ, the frequency $\omega_{c,\mu}$ is varied over μ by the filter design algorithm. In Fig. 1b the level response of a single low shelving biquad is schematically shown.
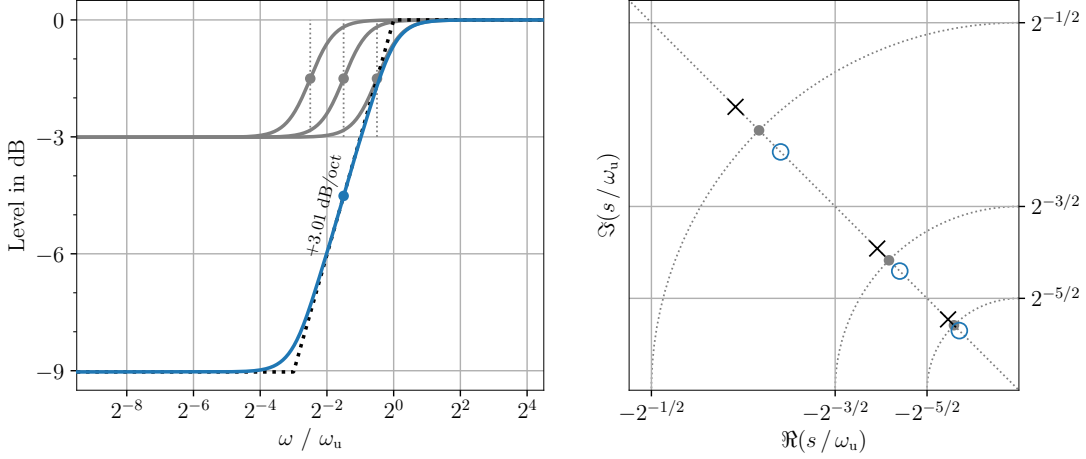
Fig. 2: Left: Level responses of the cascade of three biquads $H_\mu(s)$ (gray) building $H(s)$ (blue) with $G = -30\lg(2) \approx -9.03$ dB, $\chi = 10\lg(2) \approx +3.01$ dB/oct, $\beta = 3$ oct. Right: Corresponding poles/zeros in upper/left s-plane with linear axes scaling. Note that the conjugate-complex poles and zeros are not shown, cf. Fig. 8. Logarithmic equidistance of the poles and zeros and alignment along the line which is determined by the Q-factor is fundamental for the filter design.

B. Parameters

Based on the fundamental diffusive representation [8, Sec. 3.2], the cascade (1) allows to build shelving filters with fractional-order slopes. Particularly, the design of a shelving filter is possible, where two of the three intended parameters (cf. Fig. 1c)

- $\chi \neq 0$: transition slope in dB/oct
- $\beta > 0$: transition bandwidth in octaves
- G: shelving level in dB

can be defined by the user, determining the third one from (signs: $-$ for low shelving filter, $+$ for high shelving filter)

$$G = \mp\beta\cdot\chi, \qquad \beta = \left|\frac{G}{\chi}\right|, \qquad \chi = \mp\frac{G}{\beta}. \qquad (4)$$

For the log-log human hearing characteristics (i.e. amplitude and frequency resolution) [24], it appears reasonable to equally space the individual mid-level cutoff frequencies $\omega_{c,\mu}$ on a logarithmic frequency axis. Thus, a user definable parameter is the number of cascaded biquads per octave N_O.

The mid-level cutoff frequencies of the biquads in the cascade (1) may then be stated as

$$\omega_{c,\mu} = 2^{-(\mu+\frac{1}{2})/N_O}\cdot\omega_u \qquad (5)$$

with a user definable upper cutoff frequency ω_u in rad/s of the shelving filter cascade $H(s)$. From the intended bandwidth β the lower cutoff frequency of $H(s)$ reads

$$\omega_l = 2^{-\beta}\cdot\omega_u, \qquad (6)$$

which can be rewritten to

$$\beta = \log_2\frac{\omega_u}{\omega_l}. \qquad (7)$$

In Fig. 1c the level response is schematically shown with the introduced variables. The shelving level is equal for each biquad $H_\mu(s)$ and is given by

$$G_B = -\frac{\chi}{N_O} \qquad (8)$$

in dB. For the user defineable number of biquads N_O per octave, the total number of required biquads N for the whole cascade is derived as

$$N = \lceil\beta\cdot N_O\rceil \qquad (9)$$

with the ceiling operation $\lceil\cdot\rceil$ yielding nearest larger integer.

III. ANALOG FILTER PROPERTIES

Other than typical shelving filters, where shelving level determines the slope characteristics, the proposed filter cascade allows for adjustable slope and bandwidth. This is exemplarily demonstrated in the following. All plots use the normalized frequency ω/ω_u, therefore the upper cutoff frequency of the shelving filter cascade ω_u needs no explicit definition.

A. Working Principle

In Fig. 2 the working principle of the filter is shown with a cascade of $N = 3$ biquads and $N_O = 1$ biquad per octave. The parameter triplet is chosen to $G = -30\lg(2) \approx -9.03$ dB, $\chi = 10\lg(2) \approx +3.01$ dB/oct and $\beta = 3$ oct. According to (8), the biquad shelving level is $G_B = -10\lg(2) \approx -3.01$ dB. Butterworth factor $Q = 1/\sqrt{2}$ [25, p.792] is used. The Laplace transfer functions can be calculated with the formulas given in Sec. II. The left plot of Fig. 2 depicts the level responses of the individual biquads (gray, cf. Fig. 1b), of the shelving filter cascade (blue, cf. Fig. 1c), and the ideal piecewise linear level response (dotted black line). Due to chosen $N_O = 1$, the mid-level cutoff frequencies $\omega_{c,\mu=0,1,2}$ are distributed by integer octaves. The right plot in Fig. 2 shows the poles and zeros that

lie in the upper-left s-plane. In total, six poles and six zeros (three 2nd order sections each with a conjugate-complex pole and zero pair) build the shelving filter cascade. The gray dots indicate the mid-level frequencies $|s_{c,\mu}| = \omega_{c,\mu}$ for $\mu = 0, 1, 2$. With help of the circles, the values for $\omega_{c,\mu}$ can be read at $\Im(s)$-axis. Furthermore, along the line intersecting all gray dots (i.e. $\angle s = {}^3/_4\pi$ for the chosen $Q = {}^1/\sqrt{2}$), also all poles and zeros are aligned, cf. Fig. 8. This pole/zero alignment is typical and fundamental [8] for the proposed filter design, which is in contrast to the equiangular alignment used in [6], see Fig. 7.

The chosen Q-factor has impact on the achieved frequency response. Around the cutoff frequencies, varying Q has about the same impact as for a single 2nd order shelving filter. However, for the shelving filter cascade, varying Q has an impact on the slope and the bandwidth as well. Generally, increasing Q increases ripples along the slope in level and phase. Decreasing Q decreases the bandwidth, where the intended slope holds. Butterworth factor $Q = {}^1/\sqrt{2}$ and $Q = {}^5/_6$ [26, p.261] are good trade-off choices to obtain moderately damped responses at lower/upper cutoff frequencies as well as small slope ripple and valid slope bandwidth. To keep focus on other details, this issue is not further discussed here and in the remainder all filters use Butterworth factor $Q = {}^1/\sqrt{2}$.

B. Frequency Responses

In Fig. 3 different variations of the parameter triplet shall illustrate the capabilities of the shelving filter cascade. Each of the left plots shows the resulting level response in dB and each of the right plots depicts the phase response in degree. All filter cascades exhibit $N_O = 3$ biquads per octave. All chosen bandwidths are integer values. Then (9) yields the number of required biquads $N = 3 \cdot \beta$ and thus filter order $M = 2 \cdot N = 6 \cdot \beta$, which is convenient for mental calculation.

In Fig. 3a the shelving level $G = \pm 20 \lg(4) \approx \pm 12$ dB is fixed. Then either slope χ or bandwidth β can be additionally adjusted. The slopes $\chi = \mp 10 \lg(\sqrt{2}, 2, 4) \approx \mp 1.5, 3, 6$ dB/oct are adjusted yielding the bandwidths $\beta = 8, 4, 2$ octaves, respectively using (4). The somewhat laborious values for χ were used because these represent exact multiples of a first-order system slope of $\pm 20 \lg(2)$ dB/oct. With chosen G this then results in integer values for β. The depicted level responses in Fig. 3a verify the intended shelving characteristics. The phase responses indicate minimum-phase characteristics, with the generally known observations, that phase excess becomes larger the steeper the slope and the larger the shelving level. For the particular filter with 8 octave bandwidth, minimum-phase characteristics of constant ± 22.5 degrees for $\chi = \pm 10 \lg \sqrt{2} \approx \pm 1.5$ dB/oct is approximated in a large frequency band. This is expected for a quarter-differentiator/-integrator.

In Fig. 3b, $\chi = 10 \lg(2) \approx +3.01$ dB/oct is fixed. A positive slope requires a negative shelving level, which can be chosen as further adjustable parameter. Alternatively, the bandwidth as free parameter can be adjusted, which is pursued here with $\beta = 1, 2, 3, 6, 8$ octaves. With (4) this yields shelving levels

$G = -10 \lg(2) \cdot (1, 2, 3, 6, 8) \approx -(3, 6, 9, 18, 24)$ dB. The level responses clearly show the intended characteristics. The phase response shows the increasing phase excess in value and frequency bandwidth with increasing transition bandwidth. The filter with 8 octaves bandwidth approximates $+45$ deg constant minimum-phase (dotted line) for a large frequency band, resembling half-differentiator filter characteristics (ideally: $+3.01$ dB/oct slope and 45 deg phase).

In Fig. 3c the bandwidth $\beta = 6$ octaves is fixed. Either the slope or the shelving level can be additionally adjusted. Here the chosen integer levels $G = 7, 3, -4, -8$ dB yield slopes $\chi = -{}^7/_6, -{}^3/_6, +{}^4/_6, +{}^8/_6$ dB/oct, respectively. The level responses depict the expected characteristics. The phase responses exhibit similar characteristics varying in their maximum phase excess, which is linked to the shelving level and the achieved slope. Thus, again: a certain fractional-order slope involves a certain minimum phase (offset). In the case of an ideal slope over the whole frequency band, a constant phase $\angle H(\omega) = \frac{\pi}{2} \frac{\chi}{20 \lg(2) \text{dB/oct}}$ in radian results.

C. Constraints and Limitations

Naturally for approximations—in the present case a fractional-order slope is approximated with a finite number of biquads and a certain octave resolution—deviations to the ideal case are to be expected. This subsection exemplarily discusses the general limitation patterns of the proposed filter design method. In Fig. 4 these limitations are visualized. In Fig. 4a the effect of shelving level quantization is depicted. Since the parameter triplet G, β, χ influences N (which needs to be integer) and N_O, only certain β and G can be exactly realized with a chosen parameter set. Note that ω_u can be completely freely adjusted though. From (8), (9), the resulting shelving level G_r thus reads

$$G_r = G_B \cdot N = -\frac{\chi}{N_O} \cdot \lceil \beta \cdot N_O \rceil \tag{10}$$

for chosen χ, β and N_O. Only for $\beta \cdot N_O \in \mathbb{N}$ the intended shelving level is equal to the resulting level $G_r = G$. The larger the deviation $\beta \cdot N_O$ towards the next larger integer, the larger is the quantization error for the shelving level. This can be reproduced with the chosen parametrization in Fig. 4a for slope $\chi = +10 \lg(2) \approx +3.01$ dB/oct, bandwidth $\beta = {}^{19}/_6$ octaves and shelving level $G = -\chi \cdot \beta \approx -9.53$ dB. Only $N_O = 6$ biquads per octave yield integer $\beta \cdot N_O = 19$ and thus $G_r = G$. This quantization effect must be considered in practical designs and a tolerable, application dependent quantization step size must be defined by the user.

In Fig. 4b it is demonstrated that the desired slope and bandwidth is not always being achieved when the chosen parameters are set unfavorable. The intended bandwidth and slope is well approached if both rule-of-thumb conditions
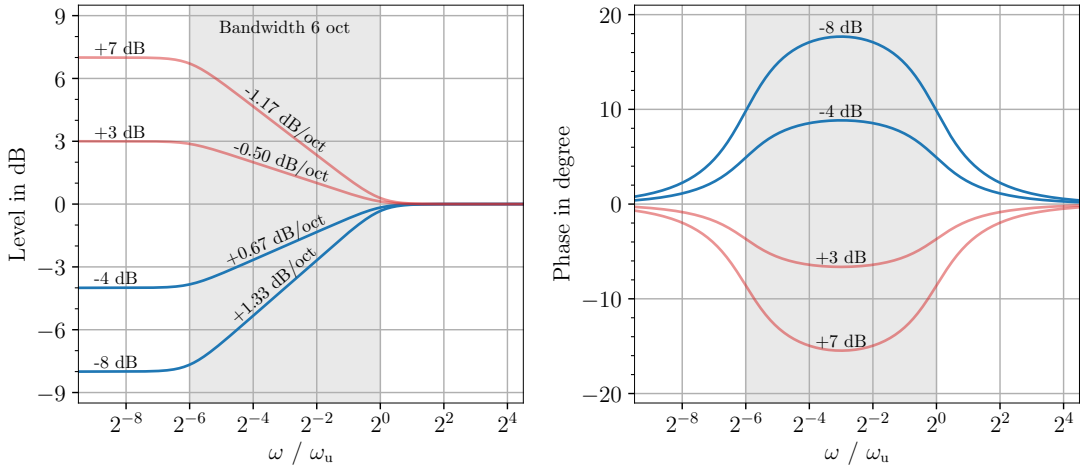
$$\beta \cdot N_O \in \mathbb{N} \tag{11}$$

$$N_O \geq \begin{cases} \frac{\chi}{12 \, \text{dB}} & \text{if } \chi \geq 12 \, \text{dB/oct} \\ 1/\text{oct} & \text{if } \chi < 12 \, \text{dB/oct} \end{cases}$$
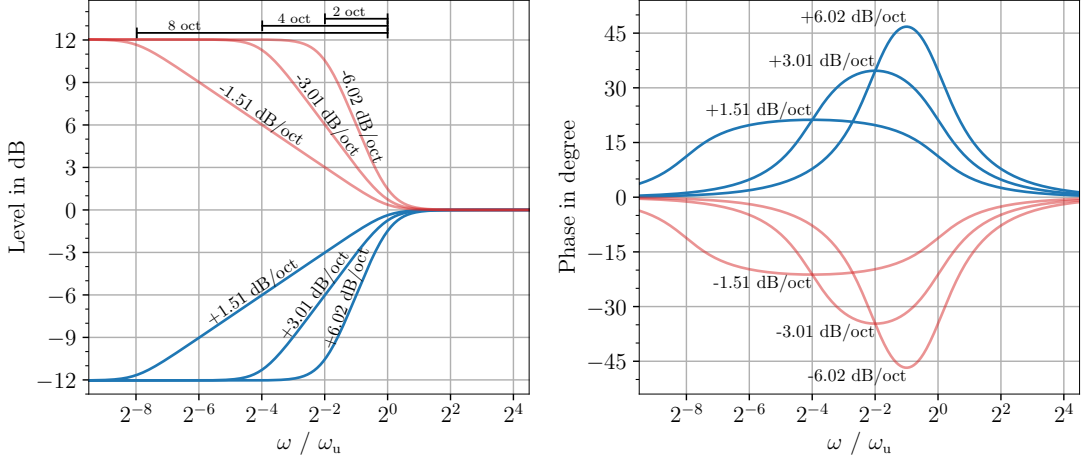
(a) Fixed shelving level $G = \pm 20 \lg(4) \approx \pm 12$ dB. Varied slope χ in dB/oct with resulting bandwidth β in octaves or vice versa.
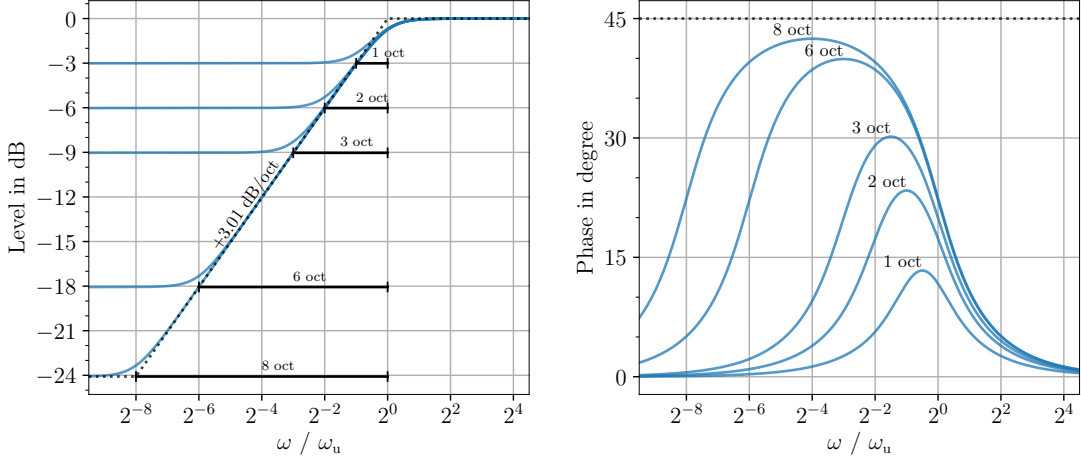
(b) Fixed slope $\chi = 10 \lg(2) \approx +3.01$ dB/oct. Varied bandwidth β in octaves, resulting shelving level G in dB or vice versa.

(c) Fixed bandwidth $\beta = 6$ octaves. Varied shelving level G in dB, resulting slope χ in dB/octave or vice versa.

Fig. 3: Shelving filter cascade frequency responses. Two of the three design parameters χ, β and G can be freely chosen, determining the third one. Depending on the target application one of the three setup strategies might be preferable.

are met at the same time, following from maximum slope of 12 dB/oct for a 2nd order filter. For Fig. 4b the parameter triplet $\chi = +120 \lg(2) \approx +36$ dB/oct, $\beta = 3$ oct, $G = -360 \lg(2) \approx -108$ dB was set up. For the chosen $N_O = 1/3, 2/3, 1, 3$ the first condition of (11) always holds, which also yields $G_r = G$, see discussion for Fig. 4a. However, only $N_O = 3$ fulfills the second condition of (11), then the resulting slope and bandwidth converge well to the intended one. For the other cases the bandwidth appears to be larger. In the extreme case of $N_O = 1/3$ only one biquad is utilized, due to $N = \lceil \beta \cdot N_O \rceil$. This single biquad obviously cannot render the intended frequency response, but rather exhibits that of a 2nd order shelving filter.

In Fig. 4c the case of slope ripple as a function of biquads per octave is discussed. As stated above, the fractional slope is approximated by biquads that are spaced with certain fractional-octave resolution. Thus it is expected, additionally to the already mentioned limitations, that the slope exhibits ripples in the level response. For Fig. 4c the parameter triplet $\beta = 9$ oct, $G = -10 \lg(2) \approx -3$ dB, $\chi = \frac{10}{9} \lg(2) \approx +0.3345$ dB/oct is set up, realized with $N_O = 2/3, 1, 3$. The condition $\beta \cdot N_O \in \mathbb{N}$ is always fulfilled, thus $G_r = G$. The choice $N_O = 2/3$ violates the 2nd condition of (11), whereas $N_O = 1, 3$ fulfill it. The deviation with respect to the ideal piecewise linear slope (cf. Fig. 1c) is visualized in terms of the error $20 \lg |H(\omega)| - 20 \lg |H_{\text{ideal slope}}(\omega)|$. It can be clearly observed as a rippled slope response. For $N_O = 2/3$ biquads per octave the ripple amounts ± 0.1 dB. For $N_O = 3$ biquads per octave the ripple becomes irrelevantly small for practical audio applications. Note that the error steeply increases at the edges of the transition band, since the resulting filter naturally deviates from the ideal piecewise linear slope. Again, one can state that the suitable amount of biquads per octave is highly dependent on the tolerated ripple. One biquad per octave resolution seems to be a good trade-off for most audio applications that ask for slopes $|\chi| < 12$ dB/oct.

In summary, all three limitations and generally $\beta \gg 1$ octave (which in practice can be relaxed to $\beta > 1$), must be taken into account by the filter designer to customize towards a target application.

IV. DISCUSSION

In this section some notes on digital filter design are given. Furthermore, a comparison to a recent cascade GEQ design is presented and potential meaningful applications are briefly outlined.

A. Digital Filter Design

So far, analog filter responses were discussed. For practical applications digital filters might be conveniently deployed instead. Digital filter design is straightforward with either the bilinear or the matched z-transform of the individual 2nd order analog filters [28–30] or as Regalia-Mitra structure with a digital allpass [5]. If the upper cutoff frequency $f_u = \frac{\omega_u}{2\pi}$ is low compared to the sampling frequency f_s, the introduced artifacts are negligible. In fact, for $f_u/f_s < \frac{1}{3}$ appropriate results are yielded, spanning almost the whole listening range for typical audio sampling frequencies. In Fig. 5 a digital shelving filter with 6 octave bandwidth and 3 dB/oct slope is depicted for $f_u = 2$ kHz and $f_s = 48$ kHz using bilinear transform without frequency pre-warping. For this example the matched z-transform practically yields the same results. Both digital filters closely match the analog target response.

### B. Comparison to Graphical Equalizer Design

GEQs can be used to approach a shelving filter characteristic with certain slope over certain bandwidth. In Fig. 6 this is exemplarily shown, deploying a very recently proposed GEQ design by Liski [27]. The filter shall have +3.01 dB/oct slope within 6 octave bandwidth with upper cutoff frequency of 2 kHz, i.e. the same as Fig. 5. The GEQ is designed from a PEQ cascade, which inherently makes constant level over a larger bandwidth an ambitious task. Thus, compared to the shelving filter cascade, the ripple at the 9 dB constant level band is larger and the -9 dB level band is not realized at all. Furthermore, a slightly larger ripple along the slope can be observed for the GEQ by close inspection. Although, the resulting filter might be acceptable, setup of different slopes and bandwidth in a GEQ might be tedious. Thus, if explicitly requiring shelving filter characteristics, the proposed shelving filter cascade could be preferred with its simpler parameter set and more accurate response.

C. Potential Applications

The presented filter could be used in audio mixing and production, where transition bandwidth might be an additional parameter for shelving filters. The proposed filter design might improve the loudness filter of [30], where a cascade of two 1st order shelving filters was designed to compensate for equal loudness level contours. The dual-band shelving filter approach [31] could make use of the proposed filter.

Usually bass boosted target transfer functions are desired for large-scale sound reinforcement, which can be conveniently realized with the proposed filter design. Furthermore, also so called line *array morphing* [32] can be approached with either varying the shelving level and the slope (Fig. 3a) or varying the level and the bandwidth (Fig. 3c).

As another example, for wave field synthesis (WFS) [33] and line source array (LSA) applications, a shelving filter with a +3 dB/oct rising slope, ideally with +45 degree phase, for the mid-frequency band is required in order to equalize the inherent acoustic lowpass characteristic of the deployed line source. The proposed filter design can be straightforwardly parametrized to obtain this commonly known WFS pre-filter and LSA coupling filter. The frequency responses shown in Fig. 3b and Fig. 5 are typical examples for it. The lower shelf compensates for the loudspeaker array's omni-directional characteristic at lower frequencies, where array length determines the lower cutoff frequency [11]. The upper shelf compensates for spatial aliasing energy [10], here upper cutoff frequency is varied to match the different spatial aliasing cutoff frequencies of sound field synthesis (SFS) methods [34]. Furthermore, dynamically
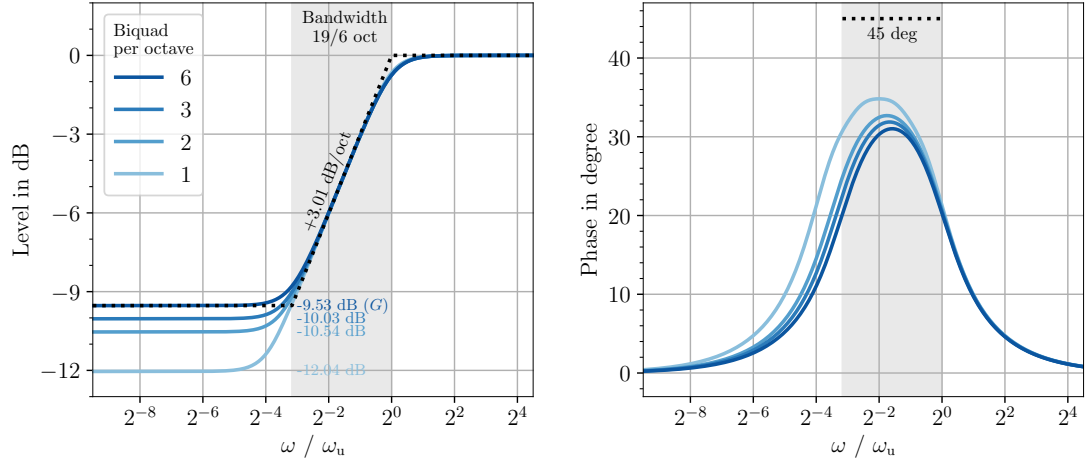
(a) Slope $\chi = 10 \lg(2) \approx +3.01$ dB/oct and shelving level $G = -\frac{19}{6} \cdot \text{oct} \, \chi \approx -9.53$ dB yields a bandwidth of $\beta = 19/6$ octaves. The resulting shelving level deviates from G for less than $N_O = 6$ biquads per octave.
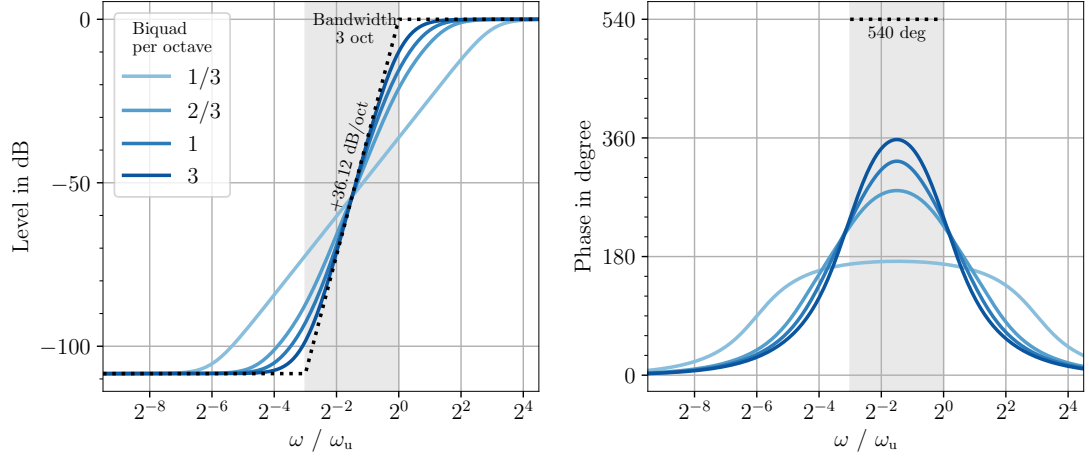
(b) Slope $\chi = 120 \lg(2) \approx +36$ dB/oct and bandwidth $\beta = 3$ octaves yields shelving level $G = -360 \lg 10(2) \approx -108$ dB. The resulting bandwidth deviates from β when deploying less than $N_O = 3$ biquads per octave.
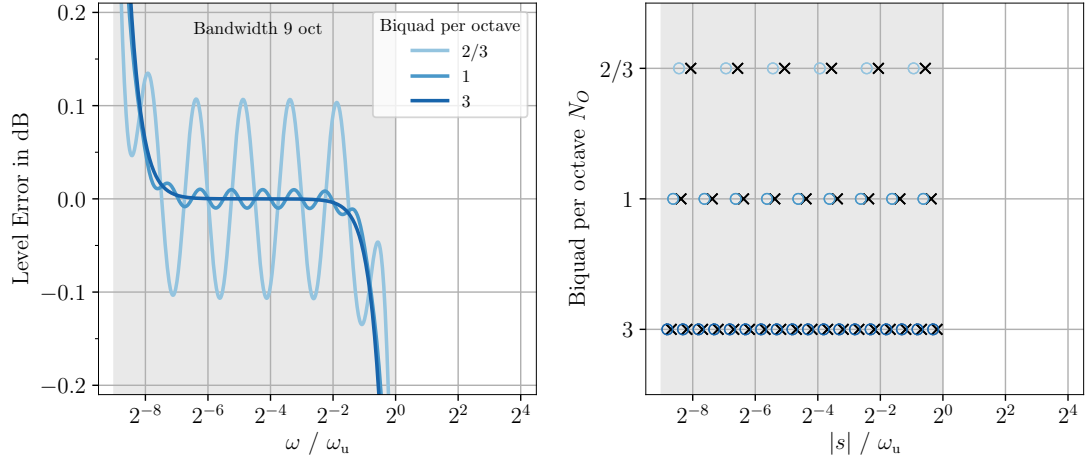
(c) $\beta = 9$ oct, $G = -10 \lg(2) \approx -3$ dB yields $\chi = \frac{10}{9} \lg(2) \approx +0.3345$ dB/oct. Left: $20 \lg |H(\omega)| - 20 \lg |H_{\text{ideal slope}}(\omega)|$. Right: distribution of poles (x) and zeros (o).

Fig. 4: Shelving filter cascade frequency responses. Limitations of the filter design method occur due to the discrete number of cascaded biquads to represent a fractional-order filter slope.
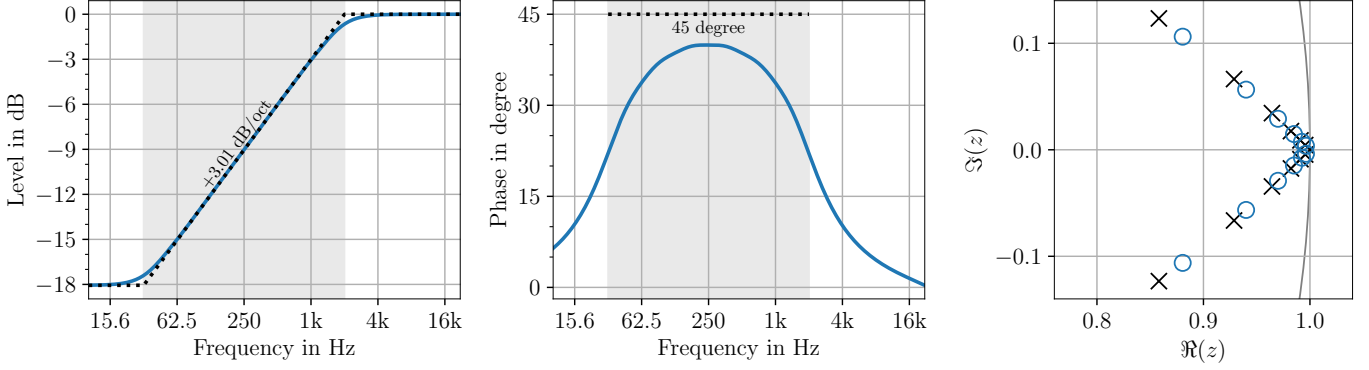
Fig. 5: Digital shelving filter cascade with bilinear z-transform for $\chi = 10\lg(2) \approx 3.01$ dB/oct and bandwidth $\beta = 6$ octaves, upper cutoff frequency 2 kHz, sampling frequency 48 kHz, $N_O = 1$ biquad per oct. Left: level response, middle: phase response, right: poles/zeros in z-plane.
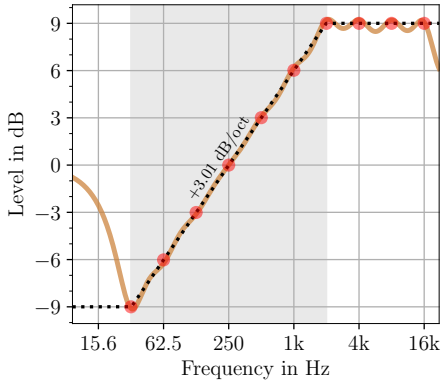

Fig. 6: Digital GEQ [27] with $f_s = 48$ kHz. The same shelving slope and bandwidth as in Fig. 5 is intended by setting the faders (red dots) accordingly. GEQ has one octave resolution to be comparable with Fig. 5

changing the filter parameters is straightforward and could be advantageously deployed for dynamic SFS, such as WFS of moving sources [35]. For SFS of focused point sources, filter responses with two different (fractional-order) slopes are required [36, 37]. This could be realized with an optimized shelving filter cascade that exhibits multiple slopes.

Multiple slope filters, or more generally multiband EQ design is out of scope of this paper. However, the band-shelving filter concept of [6] can be straightforwardly adopted for our filter design, which then could enhance the control of the transition bands with adjustable slope and bandwidth.

V. SUMMARY

This paper proposes a cascade of second-order shelving filters to realize a higher-order shelving filter with adjustable transition slope and adjustable transition bandwidth additionally to the common parameters cutoff frequency and shelving level. As a natural choice regarding human hearing, the mid-level frequencies of the biquads are equidistantly aligned with respect to logarithmic frequency axis. Thus, a critical parameter is the

number of biquads per octave, which must be sufficiently high to achieve the intended frequency response, most important a ripple free shelving slope. Digital filter design for audio applications can be straightforwardly realized with bilinear or matched-z transform of individual biquads. This IIR filter based design might be preferably used for specific applications rather than specialized FIR designs or GEQs. With its simple parametrization, the filter could be deployed in various audio applications.

APPENDIX: LAPLACE TRANSFER FUNCTION OF TRADITIONAL SHELVING FILTERS

The transfer function of a general 2nd order filter for real signals reads

$$\tilde{H}(s) = \frac{b_2 s^2 + b_1 s + b_0}{a_2 s^2 + a_1 s + a_0} \qquad (12)$$

for Laplace domain $s = \sigma + \mathrm{j}\omega$ with $b, a \in \mathbb{R}$. For $s = \mathrm{j}\omega$ the frequency response $\tilde{H}(\omega) = |\tilde{H}(\omega)|\mathrm{e}^{\mathrm{j}\angle\tilde{H}(\omega)}$ over angular frequency ω is evaluated.

The shelving filter is parametrized with shelving level G_B in dB, mid-level cutoff frequency ω_c in rad/s and—for the 2nd order filter—the pole/zero $Q \geq \frac{1}{2}$ factor (the same Q for pole and zero is applied here for convenience). With $g_B = 10^{|G_B|/20} > 0$ the coefficients for 1st/2nd order low-/high-shelving filters can be given in the following listing, cf. [23]. The $\pm$ exponent for g_B corresponds to the sign of G_B, i.e. positive or negative shelving level G_B.

The 1st order low-shelving filter is given by the coefficients for (12)

$$b_2 = 0, \quad b_1 = \frac{1}{\omega_c}, \quad b_0 = g_B^{\pm\frac{1}{2}}, \qquad (13)$$

$$a_2 = 0, \quad a_1 = \frac{1}{\omega_c}, \quad a_0 = g_B^{\mp\frac{1}{2}}.$$
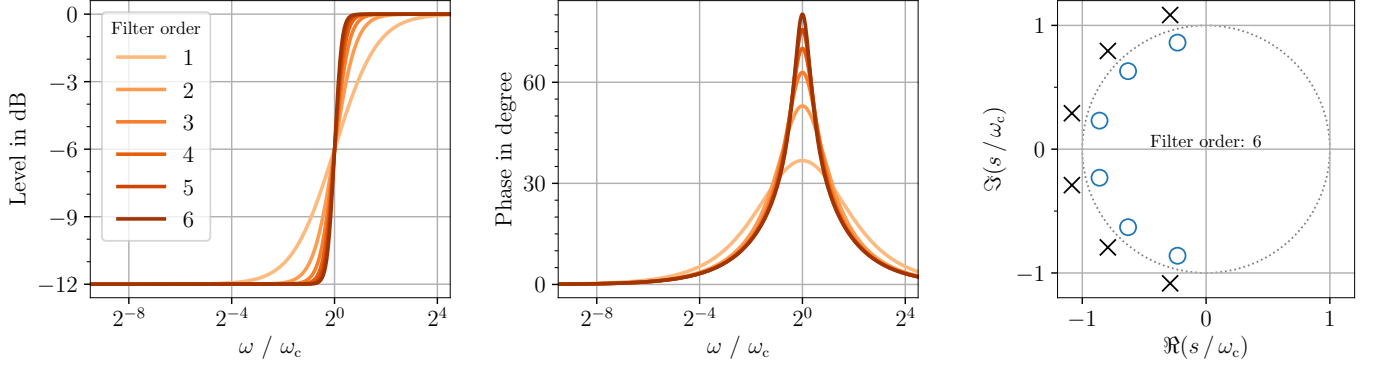
Fig. 7: Higher order low-shelving filters from Holters [6] adapted to ω_c as mid-level cutoff frequency. Then, poles and zeros are equiangularly aligned along the circle with radius $|s| = \omega_c$. The larger the filter order the closer the poles and zeros are aligned to that circle, cf. 2nd order filter pole/zero-map in Fig. 8. An increasing slope and phase excess can be observed for increased filter order, however no explicit control of transition bandwidth is possible.

The 1st order high-shelving filter is given by

$$b_2 = 0, \quad b_1 = \frac{g_B^{\pm\frac{1}{2}}}{\omega_c}, \quad b_0 = 1, \tag{14}$$

$$a_2 = 0, \quad a_1 = \frac{g_B^{\mp\frac{1}{2}}}{\omega_c}, \quad a_0 = 1.$$

The 2nd order low-shelving filter is given by the coefficients for (12), cf. [1, (15)]

$$b_2 = \frac{1}{\omega_c^2}, \quad b_1 = \frac{g_B^{\pm\frac{1}{4}}}{Q\,\omega_c}, \quad b_0 = g_B^{\pm\frac{1}{2}}, \tag{15}$$

$$a_2 = \frac{1}{\omega_c^2}, \quad a_1 = \frac{g_B^{\mp\frac{1}{4}}}{Q\,\omega_c}, \quad a_0 = g_B^{\mp\frac{1}{2}}.$$

The 2nd order high-shelving filter is given by

$$b_2 = \frac{g_B^{\pm\frac{1}{2}}}{\omega_c^2}, \quad b_1 = \frac{g_B^{\pm\frac{1}{4}}}{Q\,\omega_c}, \quad b_0 = 1, \tag{16}$$

$$a_2 = \frac{g_B^{\mp\frac{1}{2}}}{\omega_c^2}, \quad a_1 = \frac{g_B^{\mp\frac{1}{4}}}{Q\,\omega_c}, \quad a_0 = 1.$$

The 2nd order filter can be further discussed with the pole-zero map shown in Fig. 8. The zeros and poles of a 2nd order low-shelving filter are

$$s_0 = \omega_c\, g_B^{\pm\frac{1}{4}}\, e^{j\alpha} \qquad s_\infty = \omega_c\, g_B^{\mp\frac{1}{4}}\, e^{j\alpha}, \tag{17}$$

and the respective complex conjugates s_0^* and s_∞^*. The sign in the exponents is again determined by the shelving level G_B. The polar angle α in the complex s-plane (Laplace domain) relates to the Q-factor

$$Q = \frac{-1}{2\cos\alpha}. \tag{18}$$

For stable and causal filters, the poles must be in the left-half s-plane $\Re(s_\infty) < 0$, hence requiring $\frac{\pi}{2} < \alpha < \frac{3\pi}{2}$. The corresponding Q-factor is always positive and varies within $[\frac{1}{2}, \infty)$. This paper mainly considers Butterworth [25] $Q = \frac{1}{\sqrt{2}}$,

which yields $\alpha = \frac{3}{4}\pi$ as illustrated in Fig. 8. If $Q = \frac{1}{2}$, i.e. $\alpha = \pi$, the poles and zeros lie on the real axis, thus double real poles $s_0 = s_0^*$ and $s_\infty = s_\infty^*$ are obtained. In this case the 2nd order frequency response is identical to that of the 1st order shelving filter, although obtained by different pole/zero-configurations. Thus, it is sufficient to discuss the present filter design based on 2nd order filters.

In the case of high-shelving filters, the poles and zeros are exchanged. Notice that a high-shelving filter with a shelving gain $\pm g_B$ has the same poles and zeros as the low-shelving filter with $\mp g_B$. The system functions only differ by a scaling factor of $\pm g_B$ due to the leading coefficients b_2 and a_2. The scaling factor is lost information in a pole-zero map, unless
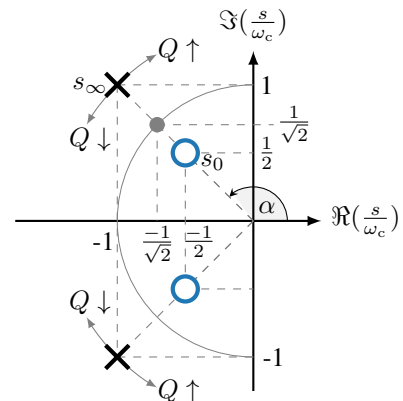

Fig. 8: Pole-zero map of 2nd order low-shelving filter with shelving level $G_B = -20\lg(4)$ dB and $Q = 1/\sqrt{2}$. The mid-level cut-frequency ω_c is represented as modulus of the gray dot $\sqrt{|s_\infty||s_0|}$. Shifting poles and zeros along the lines away from $|s| = \omega_c$ yields $g_B \uparrow$. Shifting poles and zeros towards $|s| = \omega_c$ yields $g_B \to 1$. Poles and zeros are reversed for positive shelving level $G_B > 0$ dB. The damping characteristic is controlled by rotating all poles and zeros around origin by α.

explicitly stated.

VI. References

[1] V. Välimäki and J. D. Reiss, "All About Audio Equalization: Solutions and Frontiers," *Appl. Sci.*, vol. 6, p. 129, 2016.

[2] H. Kimball, *Motion Picture Sound Engineering*, 3rd ed. New York: D. Van Nostrand, 1938, ch. XVI: Attenuation Equalizers, pp. 228–272.

[3] U. Zölzer, *DAFX: Digital Audio Effects*, 2nd ed. Chichester: Wiley, 2011.

[4] J. D. Reiss and A. P. McPherson, *Audio Effects: Theory, Implementation and Application*. Boca Raton: CRC Press, 2015.

[5] J.-M. Jot, "Proportional Parametric Equalizers—Application to Digital Reverberation and Environmental Audio Processing," in *Proc. 139th Audio Eng. Soc. Conv.*, no. #9358, New York, 2015.

[6] M. Holters and U. Zölzer, "Parametric Recursive Higher-Order Shelving Filters," in *Proc. 120th Audio Eng. Soc. Conv.*, no. #6722, Paris, 2006.

[7] D. McGrath, J. Baird, and B. Jackson, "Raised Cosine Equalization Utilizing Log Scale Filter Synthesis," in *Proc. 117th Audio Eng. Soc. Conv.*, no. #6257, San Francisco, 2004.

[8] T. Hélie, "Real-Time Simulation of a Family of Fractional-Order Low-Pass Filters," in *Proc. 135th Audio Eng. Soc. Conv*, no. #8929, New York, 2013.

[9] A. Acharya, S. Das, I. Pan, and S. Das, "Extending the Concept of Analog Butterworth Filter for Fractional Order Systems," *Sig. Process.*, vol. 94, pp. 409–420, 2014.

[10] S. Spors and J. Ahrens, "Analysis and Improvement of Pre-Equalization in 2.5-Dimensional Wave Field Synthesis," in *Proc. 128th Audio Eng. Soc. Conv.*, no. #8121, London, 2010.

[11] F. Schultz, "Sound field synthesis for line source array applications in large-scale sound reinforcement," Ph.D. dissertation, University of Rostock, 2016.

[12] J. Liski, B. Bank, J. O. Smith, and V. Välimäki, "Converting series biquad filters into delayed parallel form: Application to graphic equalizers," *IEEE Trans. Sig. Process.*, vol. 67, no. 14, pp. 3785–3795, 2019.

[13] Y. Chen and B. M. Vinagre, "A New IIR-Type Digital Fractional Order Differentiator," *Sig. Process.*, vol. 83, pp. 2359–2365, 2003.

[14] R. S. Barbosa, J. A. T. Machado, and I. M. Ferreira, "Pole-Zero Approximations of Digital Fractional-Order Integrators and Differentiators Using Signal Modeling Techniques," in *Proc. 16th World Congr. Int. Fed. Autom. Control*, Prague, 2005, pp. 309–314.

[15] ——, "Time domain design of fractional diffintegrators using least-squares," *Sig. Process.*, vol. 86, pp. 2567–2581, 2006.

[16] C.-C. Tseng and S.-L. Lee, "Closed-Form Designs of Digital Fractional Order Butterworth Filters Using Discrete Transforms," *Sig. Process.*, vol. 137, pp. 80–97, 2017.

[17] R. Whittle. (2011) DSP generation of Pink (1/f) Noise, http://www.firstpr.com.au/dsp/pink-noise/.

[18] M. Holters and U. Zölzer, "Graphic equalizer design using higher-order recursive filters," in *Proc. 9th Int. Conf. Digit. Audio Eff. (DAFx)*, Montreal, 2006, pp. 37–40.

[19] V. Välimäki and J. Liski, "Accurate cascade graphic equalizer," *IEEE Sig. Process. Letters*, vol. 24, no. 2, pp. 176–180, 2017.

[20] P. C. Eastty, "Accurate IIR Equalization to an Arbitrary Frequency Response with Low Delay and Low Noise Real-Time Adjustment," in *Proc. 125th Audio Eng. Soc. Conv.*, no. #7639, San Francisco, 2008.

[21] ——, "Audio processing," U.S. Patent #9,203,366 B2, 2015-12-01, Tech. Rep., 2015.

[22] D. Lorente, T. Meier, P. Meyer, and L. Jenks, "Filter with independently adjustable band gain and break slopes and method of constructing the same," U.S. Patent #9,722,560 B2, 2017-08-01, Tech. Rep., 2017.

[23] S. Spors. (2019) Digital Signal Processing - Lecture notes featuring computational examples, https://github.com/spatialaudio/digital-signal-processing-lecture/tree/2018/19.

[24] H. Fastl and E. Zwicker, *Psychoacoustics*, 3rd ed. Berlin: Springer, 2007.

[25] G. M. Ballou, *Handbook for Sound Engineers*, 4th ed. Burlington, MA: Focal Press, 2008.

[26] F. H. Lange, *Signale und Systeme I*, 2nd ed. Berlin: Verlag Technik, 1975.

[27] J. Liski, J. Rämö, and V. Välimäki, "Graphic equalizer design with symmetric biquad filters," in *Proc. IEEE Workshop Appl. Sig. Process. Audio Acoust. (WASPAA)*, New Paltz, 2019, pp. 55–59.

[28] E. C. Ifeachor and B. W. Jervis, *Digital Signal Processing*, 2nd ed. Essex: Prentice Hall, 2002.

[29] D. P. Berners and J. S. Abel, "Discrete-Time Shelf Filter Design for Analog Modeling," in *Proc. 115th Audio Eng. Soc. Conv.*, no. #5939, New York, 2003.

[30] S. B. Nielsen, "A Loudness Function for Analog and Digital Sound Systems based on Equal Loudness Level Contours," in *Proc. 140th Audio Eng. Soc. Conv.*, no. #9559, Paris, 2016.

[31] R. Audfray, J.-M. Jot, and S. Dicker, "Practical Realization of Dual-Shelving Filter Using Proportional Parametric Equalizers," in *Proc. 145th Audio Eng. Soc. Conv.*, no. #10054, New York, 2018.

[32] L-Acoustics, "Array morphing, V2.1," Tech. Rep., 2013.

[33] G. Firtha, P. Fiala, F. Schultz, and S. Spors, "Improved Referencing Schemes for 2.5D Wave Field Synthesis Driving Functions," *IEEE/ACM Trans. Audio Speech Language Process.*, vol. 25, no. 5, pp. 1117–1127, May 2017.

[34] F. Winter, H. Wierstorf, C. Hold, F. Krüger, A. Raake, and S. Spors, "Colouration in Local Wave Field Synthesis,"

IEEE/ACM Trans. Audio Speech Language Process., vol. 26, no. 10, pp. 1913–1924, 2018.

[35] G. Firtha, "A Generalized Wave Field Synthesis Theory with Application for Moving Virtual Sources," Ph.D. dissertation, Budapest University of Technology and Economics, 2019.

[36] S. Spors and J. Ahrens, "Local Sound Field Synthesis by Virtual Secondary Sources," in *Proc. 40th Audio Eng. Soc. Conf.*, Tokyo, 2010.

[37] S. Spors, K. Helwani, and J. Ahrens, "Local Sound Field Synthesis by Virtual Acoustic Scattering and Time-Reversal," in *Proc. 131st Audio Eng. Soc. Conv.*, no. #8529, New York, 2011.

Bibliography Comment

While discussing the work with Franz Zotter (we are as always deeply grateful), he mentioned related works

- Sophocles J. Orfanidis (2005): "High-Order Digital Parametric Equalizer Design" JAES Volume 53 Issue 11 pp. 1026-1046; November 2005
- Jonathan Abel and Julius O. Smith (2006): "Robust Design of Very High-Order Allpass Dispersion Filters". In: Proc. Conf. Digital Audio Effects (DAFx-06), Montreal, Canada

Orfanidis work is very similar to Holters/Zölzers, one could see it as a generalization for other pole/zero alignments such as Chebyshev type, whereas Abel/Smith used an IIR cascade to design allpass filters with adjustable phase.

These works from the highly appreciated colleagues unfortunately were missed in the paper, but they are very enlightening. Also, with that in mind it is very likely that the proposed filter design already existed, but it was not yet written down nicely.